

phys. stat. sol. (a) **132**, 9 (1992)

Subject classification: 61.10 and 78.70; 68.20

*Institute of Nuclear Problems, Belorussian State University, Minsk<sup>1)</sup>*

## **Fluorescence Yield under X-Ray Surface Back Diffraction**

By

S. A. STEPANOV

Peculiarities of the X-ray standing wave technique, realized under two-wave and four-wave X-ray surface back diffraction are theoretically studied. It is shown that this technique, based on the registration of the yield of X-ray fluorescence or other secondary emission from the crystal due to the dynamical surface back diffraction of X-ray radiation, can provide both coordinates parallel to the surface in the crystal unit cell for impurity atoms deposited onto the crystal surface. Worth noting is the ability of the technique proposed to fit not only perfect, but also mosaic crystals.

Теоретически анализируются возможности метода стоячих рентгеновских волн при 2-х и 4-х волновой поверхностной дифракции назад. Показано, что в этом методе, основанном на регистрации выхода флуоресценции или других вторично-эмиссионных излучений из кристалла в условиях поверхностной дифракции назад рентгеновского излучения, можно определять обе параллельные поверхности координаты в элементарной ячейке для примесных атомов, осажденных на поверхности кристалла. Особое значение имеет применимость предлагаемого метода не только для совершенных кристаллов, но и для мозаичных структур.

### **1. Introduction**

Recently, a new geometry of X-ray surface back diffraction (SBD) has been studied both theoretically and experimentally [1 to 4]. It has been shown that owing to a combination of the grazing incidence with the top Bragg angle ( $\theta_B \rightarrow 90^\circ$ ), this diffraction geometry has unique potentialities for the investigation of crystal surfaces. Particularly, using SBD, one can measure the absolute value of the lattice spacing in the crystal layer of  $\approx 1$  to 10 nm depth with an accuracy  $\Delta d/d \leq 10^{-6}$ .

In the present paper some additional possibilities for crystal surface studies are considered in relation to the realization of the X-ray standing wave technique (XRSW) under SBD. As known from [5 to 11], XRSW enables one to locate impurity atoms in the crystal unit cell from their X-ray fluorescence, which is proportional to the illumination of atoms by an X-ray standing wave, formed in a crystal under dynamical Bragg diffraction. Up to now, XRSW has been realized in three geometries of X-ray diffraction:

- I – under Bragg case diffraction (see [5] and subsequent works);
- II – under Bragg case back diffraction [6, 7];
- III – under grazing incidence (or surface) diffraction [8 to 11].

In cases I and II XRSW provides the coordinate of impurity location within crystal unit cell normal to the surface. In case III the tangential coordinate (parallel to the surface) is measured, which is of greater interest for applications. Moreover, in case III the signal-to-background ratio in surface studies is greater by a factor of  $10^2$  to  $10^3$  due to the grazing incidence. Finally, the application of XRSW in cases I and III is limited to perfect crystals

---

<sup>1)</sup> 11, Bobruiskaya st., 220080 Minsk, Belorussia.

alone, whereas in case II XRSW is free from this limitation, i.e. it allows the study of mosaic surface structures too due to the large angular scale of back diffraction, which is  $10^2$  to  $10^3$  times wider than typical diffraction peaks.

Apparently, XRSW under SBD combines the advantages of both cases II and III, i.e., to provide surface sensitivity and the tangential coordinates, on the one hand, and to be applicable to mosaic structures, on the other hand. Therefore, this technique may prove to be a new powerful tool for crystal surface studies. In this relation, Section 2 presents the theoretical analysis and computations of fluorescence yield from impurity atoms under two-wave SBD.

In Section 3 we consider the fluorescence yield under four-wave SBD and the possibilities for measuring two tangential coordinates of impurity atoms in one X-ray experiment.

## 2. Fluorescence Yield under Two-Wave SBD

As shown in [4], the dynamical diffraction equations describing SBD, are essentially the same as those describing the surface diffraction with conventional Bragg angles, except for the different angular dependences of parameter  $\alpha$ , characterizing the deviation of the incident X-ray wave from the Bragg condition. Therefore, one can evaluate the fluorescence yield under SBD, using equations from [11] for the fluorescence yield under surface diffraction and substituting therein the angular dependence of  $\alpha$  in SBD as obtained in [4].

We consider a fluorescent atom, located in the structure at a depth  $z$  at the point with the tangential vector  $\boldsymbol{\rho}_\perp$ . The fluorescence yield from this atom under two-wave SBD can be obtained from the following expression (see [11]):

$$I_{\text{fl}}(\Phi_0, \alpha, z, \boldsymbol{\rho}_\perp) \approx \left| \sum_{j=1}^2 \{D_0^{(j)} + D_h^{(j)} \exp(i\mathbf{h}\boldsymbol{\rho}_\perp + 2i\varphi k_0 z)\} \exp(ik_0 u^{(j)} z) \right|^2. \quad (1)$$

Here  $\mathbf{h}$  is the reciprocal lattice vector, making in general a small angle  $\varphi$  with the surface,  $\mathbf{k}_0$  stands for the wave vector of the incident wave,  $\Phi_0$  is the angle of incidence (see Fig. 1 a). The parameters  $D_{0,h}^{(1,2)}(\Phi_0, \alpha)$  designate the amplitudes of two transmitted and two diffracted waves, conforming to the roots  $u^{(1,2)}(\Phi_0, \alpha)$  of the dynamical diffraction dispersion equation and producing an X-ray standing wave field in the crystal. We omit here the equations for  $D_{0,h}^{(1,2)}$  and  $u^{(1,2)}$  because they are completely identical to those in [11], except that the following expression for  $\alpha$  should be used from [4]:

$$\alpha = 2\{\delta\theta^2 + (\Phi_0 + \varphi)^2 - 2\varepsilon\}. \quad (2)$$

Here  $\delta\theta$  is the azimuth diffraction angle (the angle between the projections of  $\mathbf{k}_0$  and  $\mathbf{h}$  on the crystal surface),  $\varepsilon \equiv 1 - \lambda/2d$  a small parameter, characterizing the deviation of the Bragg angle from  $90^\circ$  at back diffraction.

As follows from (2), the SBD diffraction pattern and the respective fluorescence yield depend on two angles,  $\delta\theta$  and  $\Phi_0$ . Since this dependence is a square-law on both angles, the diffraction band has a large angular scale;  $\Delta(\delta\theta, \varphi_0) \approx 10^{-3}$  to  $10^{-2}$  rad.

For definiteness, we consider the fluorescence yield from atoms located on the crystal surface ( $z = 0$ ). Conforming to (1), the dependence of fluorescence yield on the coordinates of the atom is contained in  $(\mathbf{h}\boldsymbol{\rho}_\perp) \equiv 2\pi(hx)$ . Here  $x$  is the tangential coordinate along  $\mathbf{h}$ . The second lateral coordinate  $y$ , normal to  $\mathbf{h}$ , does not affect the fluorescence intensity.

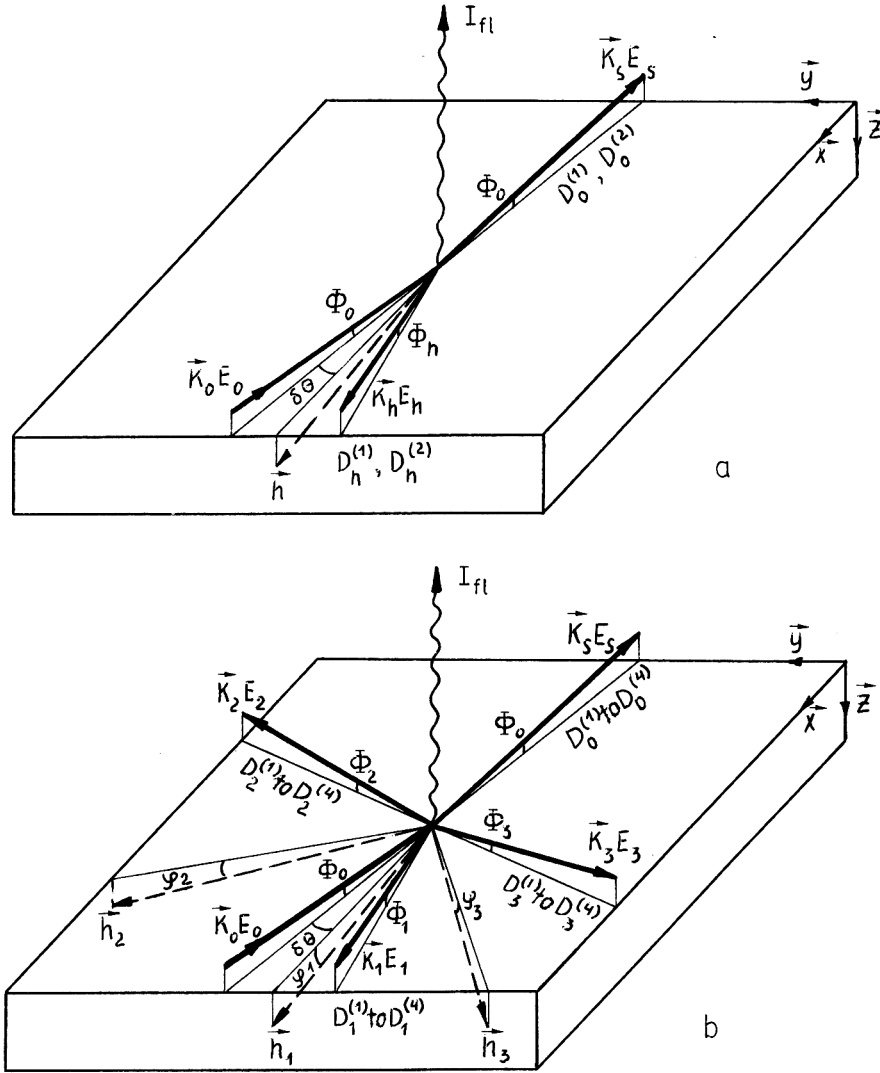


Fig. 1. Schematic representation of fluorescent yield under X-ray surface back diffraction in a) two-wave and b) four-wave cases.  $k_0$ ,  $k_s$ ,  $k_h$  stand for the wave vectors of incident, transmitted, and diffracted waves,  $h_m$  for reciprocal lattice vectors,  $E_m$ ,  $D_m^{(j)}$  are the wave field amplitudes in vacuum and inside the crystal, respectively,  $\varphi_m$  are the misorientation angles of  $h_m$ ,  $\Phi_0$ ,  $\Phi_m$  are the incident angle and the exit angles of the waves,  $\delta\theta$  is the azimuth diffraction angle

Fig. 2a, b shows the fluorescence yield  $I_{fl}(\Phi_0, \delta\theta)$  from the surface atoms having different locations with respect to the diffracting planes: a) at sites ( $hx = 0$ ) and b) at interstitials ( $hx = 1/2$ ). The computations were carried out for Ge, (620),  $\text{CoK}_{\alpha 1}$  radiation,  $\varepsilon = 4 \times 10^{-5}$ ,  $\varphi = 0$ . Fig. 2c depicts the respective pattern of the SBD reflection coefficient. The comparison of Fig. 2a, b clearly demonstrates that the two types of atom location provide substantially different fluorescence yields over a very wide angular range of  $\approx 1$  to  $2^\circ$ .

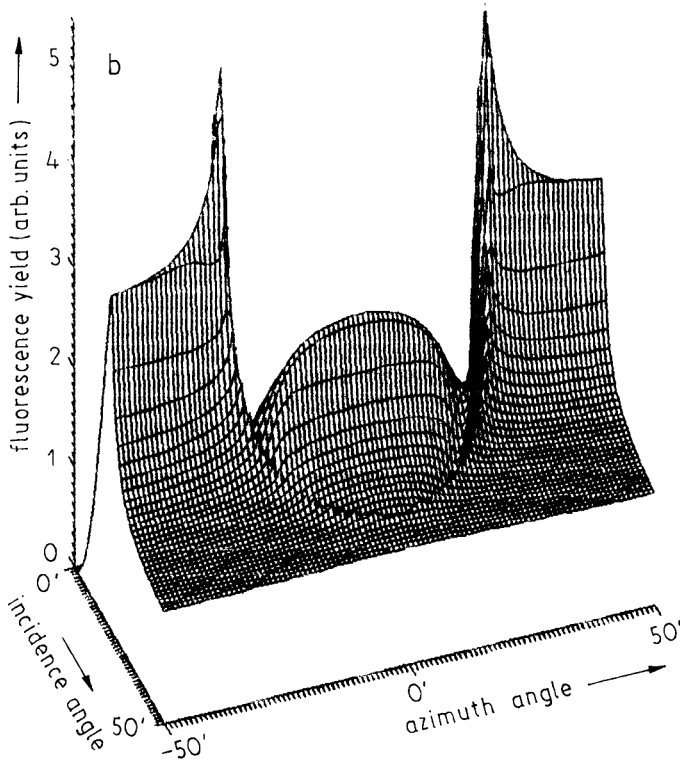
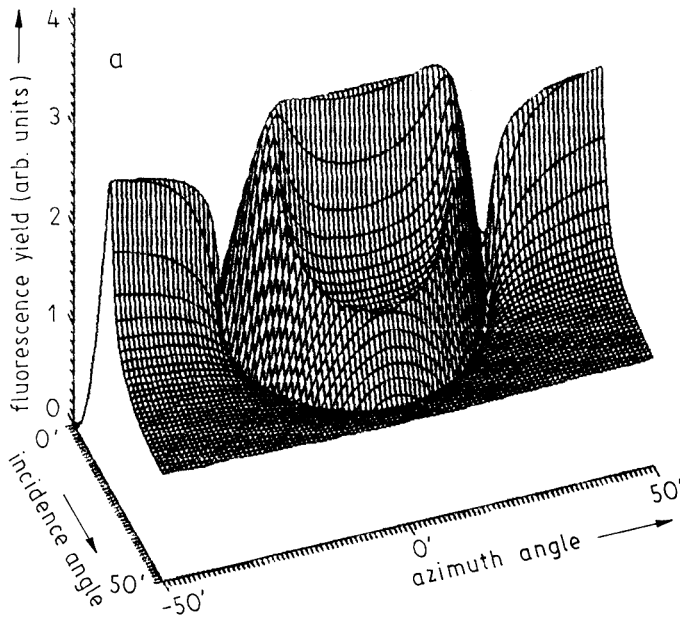


Fig. 2 a, b

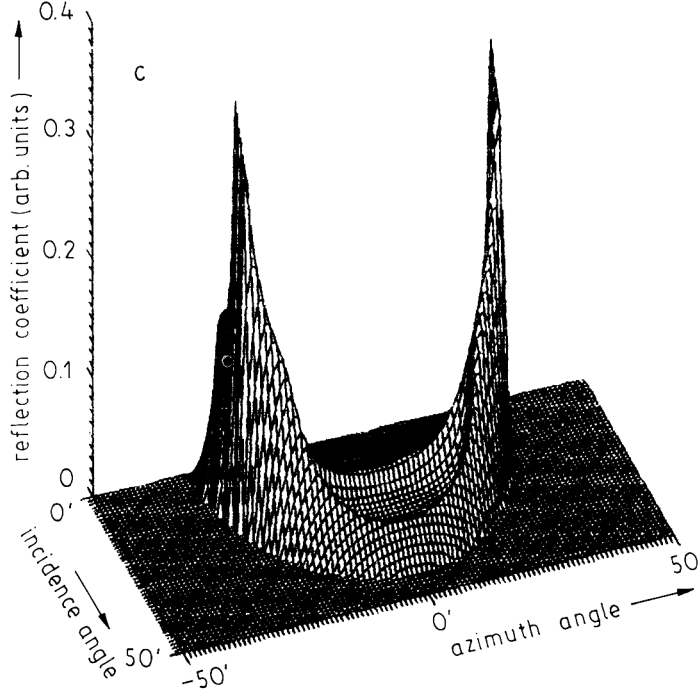


Fig. 2. Fluorescence yield from the surface atoms under SBD of  $\text{CoK}_{\alpha 1}$  radiation on the (620) planes of Ge ( $\varepsilon = 4 \times 10^{-5}$ ,  $\varphi = 0$ ). Computations were performed in a two-wave approximation. a) Fluorescent atoms lie on the diffracting planes ( $hx = 0$ ), b) midway between the diffracting planes ( $hx = 1/2$ ), c) is the respective pattern of SBD reflection coefficient

Thus, XRSW under SBD can supply the lateral coordinates of impurity atoms deposited on the crystal surface. Thanks to the large angular scale of the fluorescence pattern, this technique is applicable not only to perfect crystals, but also to mosaic structures, provided that the mosaic spread is less than  $\approx 1$  to  $2^\circ$ .

### 3. Fluorescence Yield under Four-Wave SBD

As shown in [4], the majority of the SBD cases, due to the high symmetry, are accompanied by multi-wave effects. For example, SBD on planes (620) in Ge, treated in Section 2 in two-wave approximation, is in fact a four-wave case with the excitation of additional (440) and  $(2\bar{2}0)$  reflections. At the same time, the analysis made in [4] has shown that the multi-wave nature of SBD is displayed within a very narrow angular band near  $\delta\theta = 0$  (compare the patterns (Fig. 2c and Fig. 3b), computed in two-wave and four-wave approximation, respectively).

Consider the fluorescence yield under four-wave SBD in the case, when all diffracting planes are normal to the surface, i.e., the conditions of the surface diffraction are met for all the reflections (see Fig. 1b). We shall see which additional information on the crystal surface may be extracted from the multi-wave fluorescence in this particular case.

The four-wave fluorescence intensity may be written in the form (compare with (1) and [12])

$$I_{\text{fl}}(\Phi_0, \delta\theta, z, \mathbf{q}_\perp) \approx \left| \sum_{j=1}^4 \left\{ D_0^{(j)} + \sum_{m=1}^3 D_m^{(j)} \exp(i\mathbf{h}_m \mathbf{q}_\perp + i\psi_m k_0 z) \right\} \exp(ik_0 u^{(j)} z) \right|^2. \quad (3)$$

Here  $D_0^{(j)}$  and  $D_{1,2,3}^{(j)}$  are the amplitudes of transmitted and diffracted waves in the crystal, conforming to four solutions  $u^{(j)}$  with  $\text{Im}(u^{(j)}) > 0$  of the dispersion equation (11) from [4];  $\mathbf{h}_{1,2,3}$  are the reciprocal lattice vectors,  $\varphi_m = 2\varphi_m \sin(\theta_{Bm})$ ;  $\varphi_{1,2,3}$  are the misorientation angles of  $\mathbf{h}_{1,2,3}$  with respect to the surface. For definiteness, (3) was written for a  $\sigma$ -polarized incident wave.

The right-hand side of (3) does not contain a factor characterizing the escape probability of fluorescent quanta from the crystal, since the depth of quantum formation under surface diffraction ( $\approx 1$  to 10 nm) is much less than their absorption depth, and hence all quanta escape from the crystal.

For the evaluation of  $D_0^{(j)}$ ,  $D_m^{(j)}$ , and  $u^{(j)}$  the reader is referred to [4]. Thus, (3) provides a complete description of the fluorescence yield under four-wave SBD.

Fig. 3a presents an example of four-wave fluorescence yield computation with (3). The comparison of Fig. 3a with Fig. 2a reveals that the multi-wave nature of the fluorescence yield is displayed only in the vicinity of  $\delta\theta = 0$ .

Consider the effect of the coordinates of a fluorescent atom in the crystal unit cell on the fluorescence yield in a narrow multi-wave band. Let the atom lie on the surface ( $z = 0$ ) and  $\varphi_{1,2,3} = 0$ . Then (3) transforms to the following form:

$$I_{\text{fl}}(\Phi_0, \delta\theta, z, \mathbf{q}_\perp) \approx \left| \sum_{j=1}^4 \left\{ D_0^{(j)} + \sum_{m=1}^3 D_m^{(j)} \exp(i\mathbf{h}_m \mathbf{q}_\perp) \right\} \right|^2. \quad (4)$$

The tangential coordinate vector  $\mathbf{q}_\perp$  can be resolved into two components ( $x, y$ ) parallel and normal to  $\mathbf{h}_1 \equiv \mathbf{h}_{\text{SBD}}$ , respectively,

$$\mathbf{q}_\perp = 2\pi(x\mathbf{e}_{\text{SBD}} + y\mathbf{e}_{\text{norm}}). \quad (5)$$

Then, accounting for the correlations:  $\mathbf{h}_2 \perp \mathbf{h}_3$  and  $\mathbf{h}_2 + \mathbf{h}_3 = \mathbf{h}_1$  (see [4]), we obtain

$$\begin{aligned} (\mathbf{h}_1 \mathbf{q}_\perp) &= 2\pi h_1 x, & (\mathbf{h}_2 \mathbf{q}_\perp) &= 2\pi h_1 (x \sin^2 \theta_{B2} + y'), \\ (\mathbf{h}_3 \mathbf{q}_\perp) &= 2\pi h_1 (x \sin^2 \theta_{B3} - y'), \end{aligned} \quad (6)$$

where  $y' = y \sin \theta_{B2} \sin \theta_{B3}$ ,  $\theta_{B2}$ ,  $\theta_{B3}$  are the Bragg angles.

It follows evidently from (4) to (6) that the fluorescence yield in a multi-wave angular band is sensitive to both lateral coordinates  $x$  and  $y$  of the atoms, as distinct from the two-wave case, where only  $x$ -sensitivity takes place.

Secondly, due to the  $x$ -dependence of  $(\mathbf{h}_2 \mathbf{q}_\perp)$  and  $(\mathbf{h}_3 \mathbf{q}_\perp)$ , the sensitivity of fluorescence yield to  $x$  in a multi-wave region differs from that in a two-wave region. For illustration, consider four-wave SBD on the (620) planes in Ge with the excitation of the (440) and (2 $\bar{2}$ 0) reflections. Here in the two-wave region the fluorescent atoms produce the same fluorescence pattern, if they are located in the unit cell at a spacing  $\Delta \mathbf{x} = (1/12, 1/4, 0)$ . At the same time, in the four-wave region the atoms produce the same pattern, if the spacing between them is a multiple of  $3\Delta \mathbf{x}$  (and  $\Delta \mathbf{y}'$  is a multiple of  $(1/8, -3/8, 0)$ , since only at such spacings both  $(\mathbf{h}_2 \Delta \mathbf{q}_\perp)$  and  $(\mathbf{h}_3 \Delta \mathbf{q}_\perp)$  are multiples of  $2\pi$ .

Based on the above consideration, we can propose a technique for obtaining the two lateral coordinates of impurity location on the crystal surface by one XRSW measurement, taken under multi-wave SBD. In this technique the  $x$ -coordinate is obtained from the analysis of the fluorescence pattern shape in the two-wave region, and then the  $y$ -coordinate is determined by analyzing the shape in the central multi-wave band. The effect of the  $y$ -coordinate of the atoms on the fluorescence yield in the central multi-wave band at different  $x$  is shown in Fig. 4.

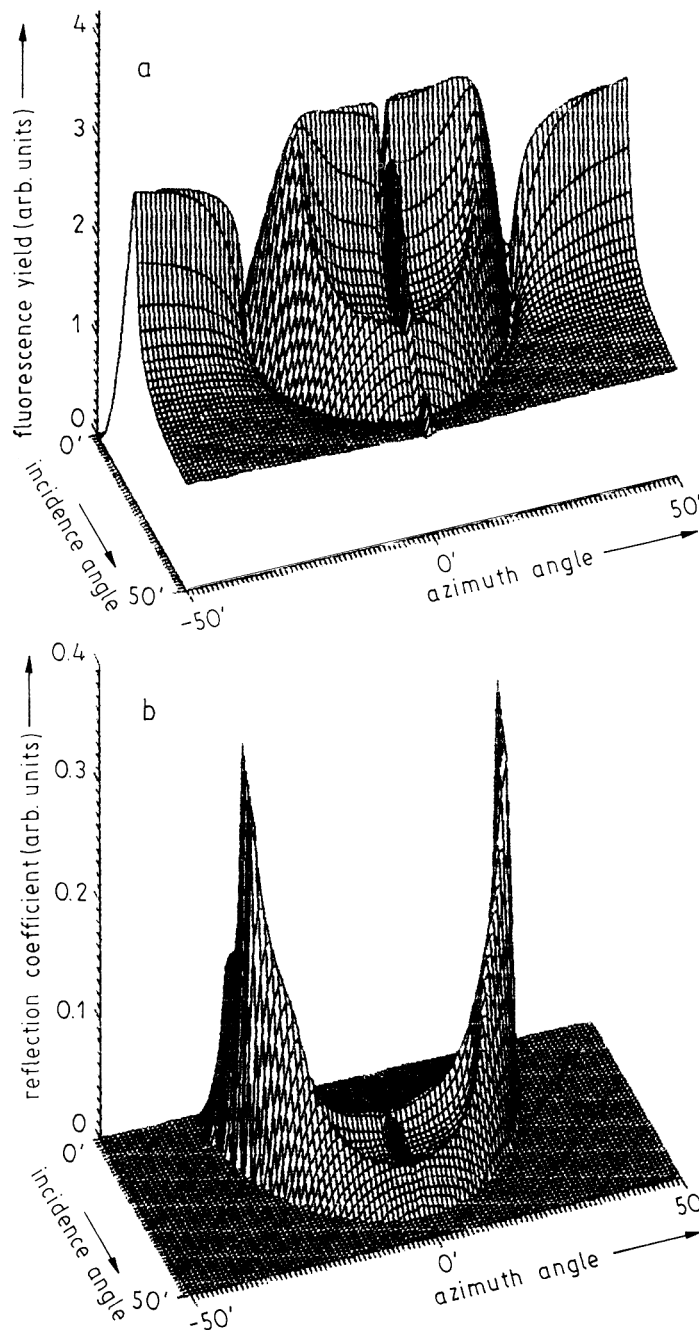


Fig. 3. The same as in Fig. 2, but computations were performed in a four-wave approximation with accounting for the excitation of  $(440)$  and  $(2\bar{2}0)$  reflections. a) Fluorescent atoms lie at the point of intersection of the three diffracting planes ( $h_i q_{\perp} = 0$ ), b) is the respective pattern of the four-wave SBD

It is evident that the proposed multi-wave technique will not be suitable for mosaic structures, since the narrow multi-wave pattern will be spread. In this case  $x$  and  $y$  can be obtained through measurements of a few two-wave fluorescence patterns, taken for two nonparallel SBD reflections.

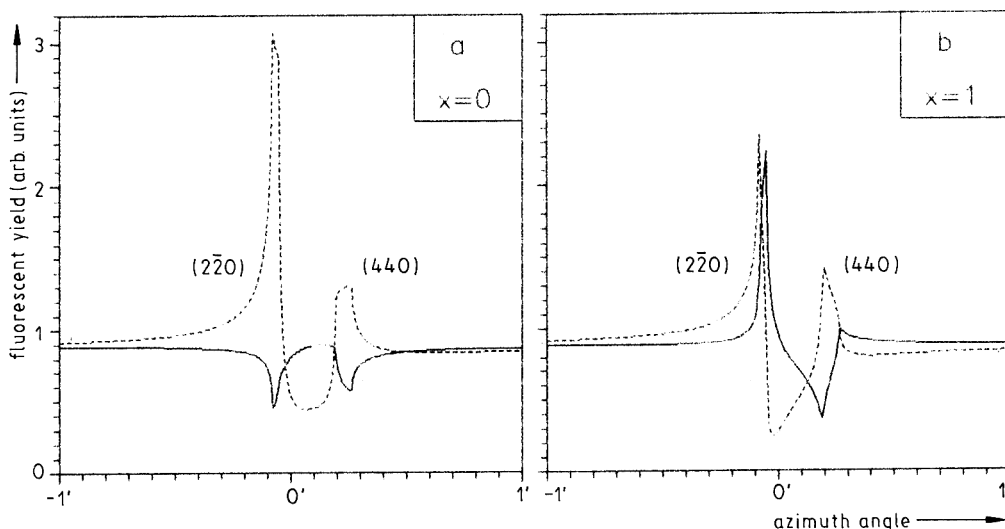


Fig. 4. Four-wave fluorescence yield as a function of azimuth diffraction angle for different tangential coordinates  $x$  and  $y$  of fluorescent surface atoms. Computations were carried out for  $\Phi_0 = 10^\circ$ ; the other parameters were the same as in Fig. 2, 3. a)  $x = 0$ , b)  $x = 1$ . Solid lines correspond to  $y' = 0$ , dashed lines to  $y' = 1/2$

In conclusion, it should be noted that the above considerations can be applied not only to fluorescence yield, but also to other secondary emissions (for example, to Auger electrons).

The author believes that the proposed techniques for measuring impurity coordinates on the crystal surface could find wide application in surface studies. He is willing to cooperate with colleagues, who are interested in the implementation of the proposed experiments.

### References

- [1] S. A. STEPANOV, E. A. KONDRASHKINA, and D. V. NOVIKOV, Collect. Abstr. XII Europ. Crystallography Meeting, Vol. 3, Moscow 1989 (p. 104).
- [2] D. V. NOVIKOV, E. A. KONDRASHKINA, and S. A. STEPANOV, phys. stat. sol. (a) **114**, K7 (1989).
- [3] E. A. KONDRASHKINA, D. V. NOVIKOV, and S. A. STEPANOV, phys. stat. sol. (a) **121**, K9 (1990).
- [4] S. A. STEPANOV, E. A. KONDRASHKINA, and D. V. NOVIKOV, Nuclear Instrum. and Methods **A301**, 350 (1991).
- [5] P. L. COWAN, J. A. GOLOVCHENKO, and M. F. ROBINS, Phys. Rev. Letters **44**, 1680 (1980).
- [6] D. P. WOODRUFF, D. L. SEYMOUR, C. F. MCCONVILLE, C. E. RILEY, M. D. CRAPPER, N. P. PRINCE, and R. G. JONES, Phys. Rev. Letters **58**, 1460 (1987); Surface Sci. **195**, 237 (1988).
- [7] H. HASHIZUME and T. NAKAHATA, Japan. J. appl. Phys. **27**, L1568 (1988).
- [8] A. M. AFANASEV, R. M. IMAMOV, E. KH. MUKHAMEDZHANOV, and V. M. PEREGUDOV, phys. stat. sol. (a) **98**, 367 (1986).
- [9] P. L. COWAN, S. BRENNAN, T. JACH, M. J. BEDZIK, and G. MATERLIK, Phys. Rev. Letters **57**, 2399 (1986).
- [10] A. M. AFANASEV, R. M. IMAMOV, A. V. MASLOV, and E. KH. MUKHAMEDZHANOV, phys. stat. sol. (a) **113**, K153 (1988).
- [11] V. G. BARYSHEVSKII and S. A. STEPANOV, phys. stat. sol. (a) **122**, 69 (1990).
- [12] V. G. KOHN, phys. stat. sol. (a) **106**, 31 (1988).

(Received February 20, 1992)